Computer Simulation - Challenge of Self Assembly

Michael L. Klein
University of Pennsylvania

Takeuchi, Seijiro
Okayama

UNITED STATES DEPARTMENT OF COMMERCE
Maurice H. Stans, *Secretary*
NATIONAL BUREAU OF STANDARDS • A. V. Astin, *Director*

Molecular Dynamics and Structure of Solids

Edited by
R. S. Carter and J. J. Rush

Institute for Materials Research
National Bureau of Standards
Washington, D.C. 20234

Based on Invited and Contributed Papers
2nd Materials Research Symposium
held at the NBS, Gaithersburg, Maryland
October 16–19, 1967

National Bureau of Standards Special Publication 301

Nat. Bur. Stand. (U.S.), Spec. Publ. 301, 571 pages, (June 1969)
CODEN: XNBSA

Issued June 1969

ON THE SECOND ORDER ELASTIC CONSTANTS OF MOLECULAR SOLIDS

M. L. KLEIN*

School of Chemistry
University of Bristol, Bristol, England

In this paper we are concerned with the possible importance of anharmonic effect in the interpretation of the thermoelastic properties of molecular solids. In particular, we shall be concerned with the relationship between elastic constants determined by

(a) Isothermal thermodynamic measurement
(b) Velocity of ultrasound (adiabatic)
(c) Slopes of phonon dispersion curves as measured by the inelastic scattering of neutrons.

For a strictly harmonic solid these three measurements are equivalent and simply related to the harmonic force constants. However, in an anharmonic crystal (i.e., real crystal) these three quantities, in principle at least, show a different temperature dependence. Later we shall use solid Kr to illustrate the posible magnitude of these differences. Solid Kr is chosen because it is a crystal in which anharmonic effects are important, but not dominant, and this situation is likely to be common to many other molecular solids.

1. Isothermal Elastic Constants

Here it is convenient to define isothermal elastic constants as the coefficients in the Taylor series expansion of $(F/\mathring{V})$, the Helmoltz free energy density, in powers of the homogeneous strain parameters $\{u_{\alpha\beta}\}$.

$$(F-\mathring{F})/\mathring{V}=S_{\alpha\beta}u_{\alpha\beta}+\frac{1}{2}S^{\text{iso}}_{\alpha\beta\sigma\tau}u_{\alpha\beta}u_{\sigma\tau}$$

Thus
$$\mathring{V}S^{\text{iso}}_{\alpha\beta\sigma\tau}=(\partial^2 F/\partial u_{\alpha\beta}\partial u_{\sigma\tau})_T$$

Since the Helmholtz energy is temperature dependent, so too are the isothermal elastic constants. In particular the lowest order explicit temperature dependence is given by

$$(1/\mathring{V})\sum_{qj}[\beta_{\alpha\beta\sigma\tau}e-\gamma_{\alpha\beta}\gamma_{\sigma\tau}Tc_v]$$

*ICI Fellow.

Crystal Structure and Pair Potentials: A Molecular-Dynamics Study

M. Parrinello[a] and A. Rahman
Argonne National Laboratory, Argonne, Illinois 60439
(Received 31 July 1980)

With use of a Lagrangian which allows for the variation of the shape and size of the periodically repeating molecular-dynamics cell, it is shown that different pair potentials lead to different crystal structures.

$$L = \tfrac{1}{2}\sum m_i \dot{\mathbf{s}}_i' \underline{G} \dot{\mathbf{s}}_i - \sum_i \sum_{j>i} \varphi(r_{ij}) + \tfrac{1}{2} W \,\mathrm{Tr}(\dot{\underline{h}}' \dot{\underline{h}}) - p_{\mathrm{ext}} \Omega .$$

25 years ago !!

[3] D. L. Price, Phys. Rev. A 4, 358 (1971); D. L. Price, K. S. Singwi, and M. P. Tosi, Phys. Rev. B 2, 2983 (1970).

[4] J. Copley and M. Rowe, Phys. Rev. Lett. 32, 49 (1974); A. Rahman, Phys. Rev. Lett. 32, 52 (1974), have shown that the V_{Rb} of Ref. 3 gives a good model of rubidium.

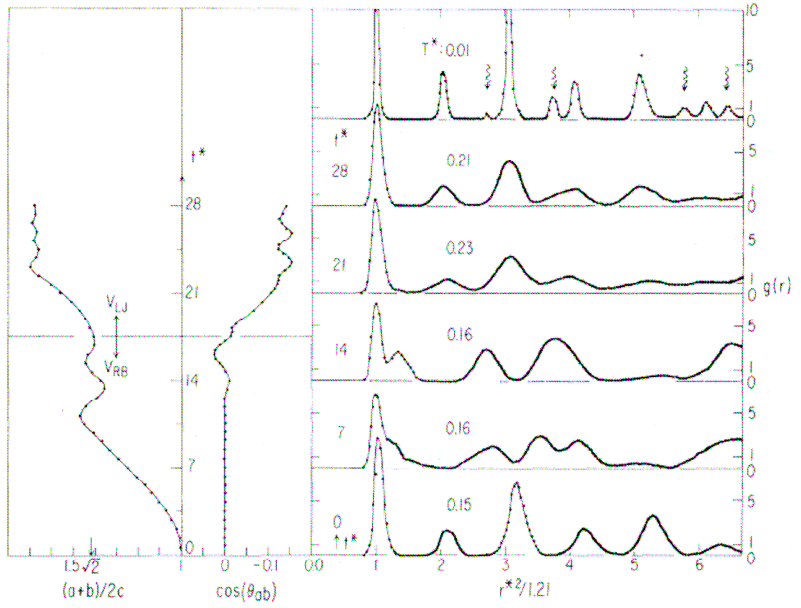

FIG. 1. The first graph on the left-hand side shows the MD cell edges $\{\vec{a}, \vec{b}, \vec{c}\}$ as a function of time t^*. The ratio $(a+b)/2c$ has been plotted; it is unity at $t^*=0$ When the potential is V_{Rb} and the MD cell is cubic; it tends to $\sqrt{2}$ with the passage of time. When V_{Rb} is changed to V_{LJ} at $t^*=17.5$, further changes occur in $\{\vec{a}, \vec{b}, \vec{c}\}$ accompanied by a change of the angle between $\vec{a}$ and $\vec{b}$. The cosine of this angle is shown as a function of time in the second graph from the left. The various times at which the $g(r)$ was monitored are indicated on the series of graphs on the right; each $g(r)$ is an average over 140 time steps; the average temperature during these time steps is also shown. The final state when quenched reveals, in the topmost figure, subsidiary peaks (wiggly arrows) due to stacking faults mentioned in the text. Note that g is plotted as a function of r^2. The ratio of the squares of shell distances is 1:2:3:4:5:6, etc., in an fcc lattice and 1:4/3:8/3:11/3:4:16/3:19/3:20/3, etc., in a bcc lattice.

A study of solid and liquid carbon tetrafluoride using the constant pressure molecular dynamics technique

Shuichi Nosé and Michael L. Klein

Chemistry Division, National Research Council of Canada, Ottawa, Canada K1A OR6
(Received 21 January 1983; accepted 24 February 1983)

The constant pressure molecular dynamics technique originally proposed by Andersen to study fluids and subsequently generalized by Parrinello and Rahman to deal with crystals of arbitrary symmetry has been further extended to treat molecular systems. As a pedagogical example designed to illustrate the utility of this approach, we have investigated the properties of carbon tetrafluoride in its condensed phases using an intermolecular potential based upon atom–atom interactions. In particular, we have explored the effect of changes in temperature and pressure on the orientationally ordered low temperature monoclinic solid. As in the real crystal, isobaric heating to sufficiently high temperature causes the ordered phase to transform spontaneously to a noncubic orientationally disordered phase. The properties of this disordered phase are also examined along with those of the liquid. The atom–atom potential appears to correlate a wide range of experimental data. The possible role of the electrostatic octopole–octopole interactions is also discussed briefly.

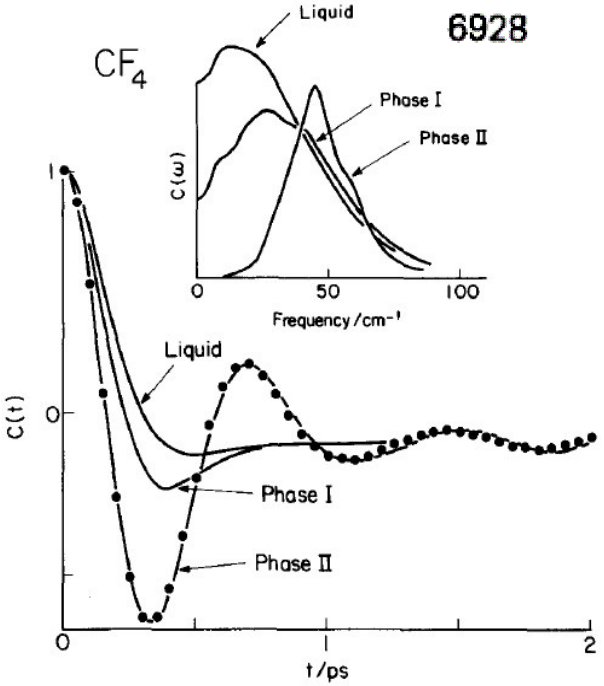

FIG. 10. The angular velocity autocorrelation function $C(t)$ and its associated power spectrum $C(\omega)$ for the three phases of CF_4. The bold lines were obtained from the constant volume MD runs listed in Table IV and the circles from the constant pressure run 1 in Table I.

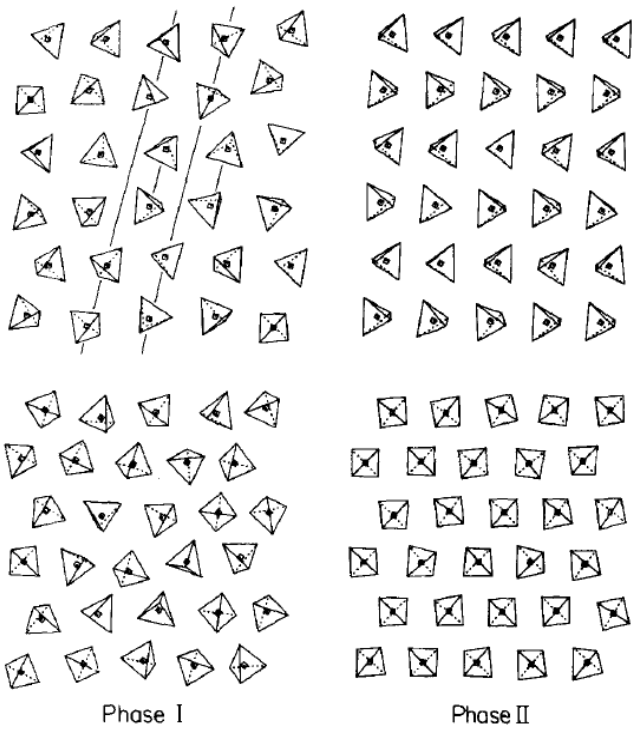

FIG. 7. Instantaneous configurations taken from MD calculations in the ordered and orientationally disordered solid phases of CF_4. The bold lines on the disordered configurations are drawn to indicate why the structural parameter $\epsilon = 0.25$.


GORDON RESEARCH CONFERENCE

Nature's Nanoworld *

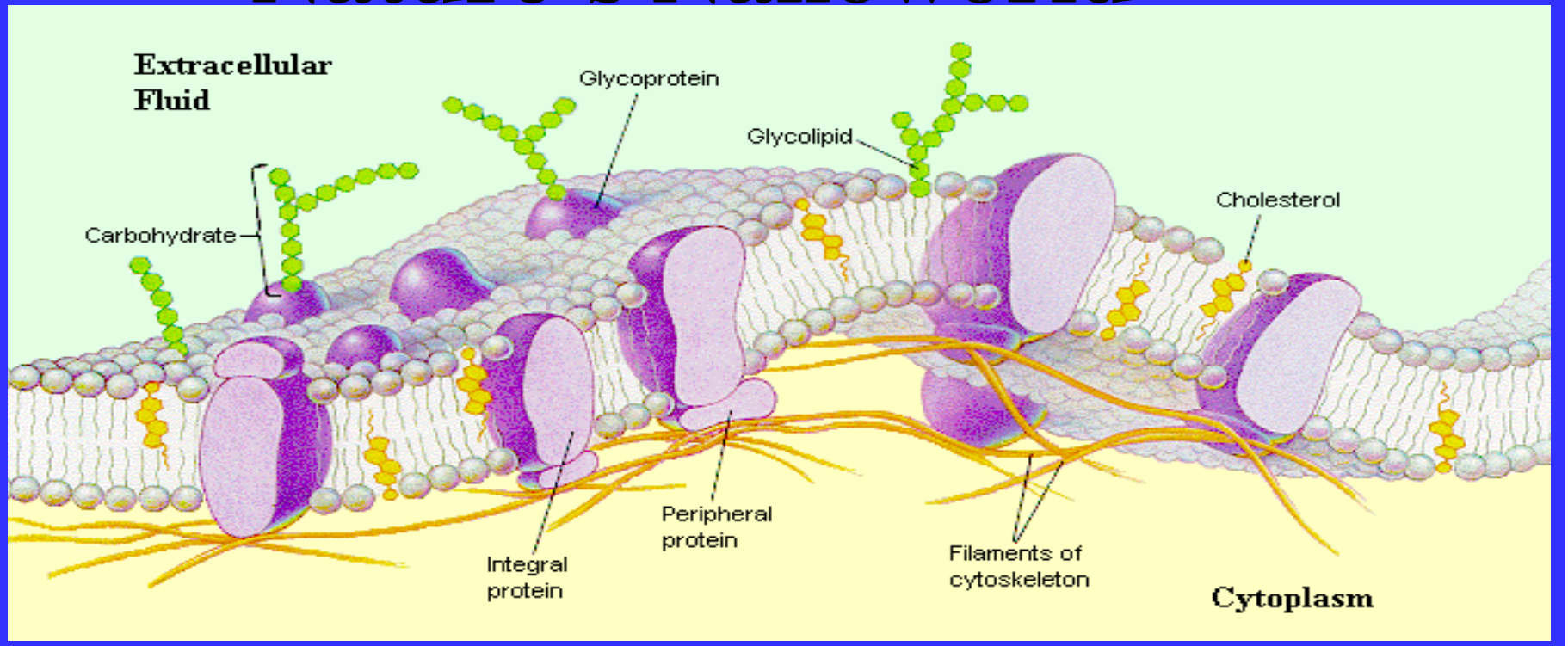

*Cell membranes are complex, containing lipids, proteins, cholesterol, carbohydrates, plus actin filements, etc… Design principles for Nature's devices, plus their self- & supramolecular assembly can yield new materials.

Membrane Bilayer Modeling

Fully hydrated DPPC bilayer structure

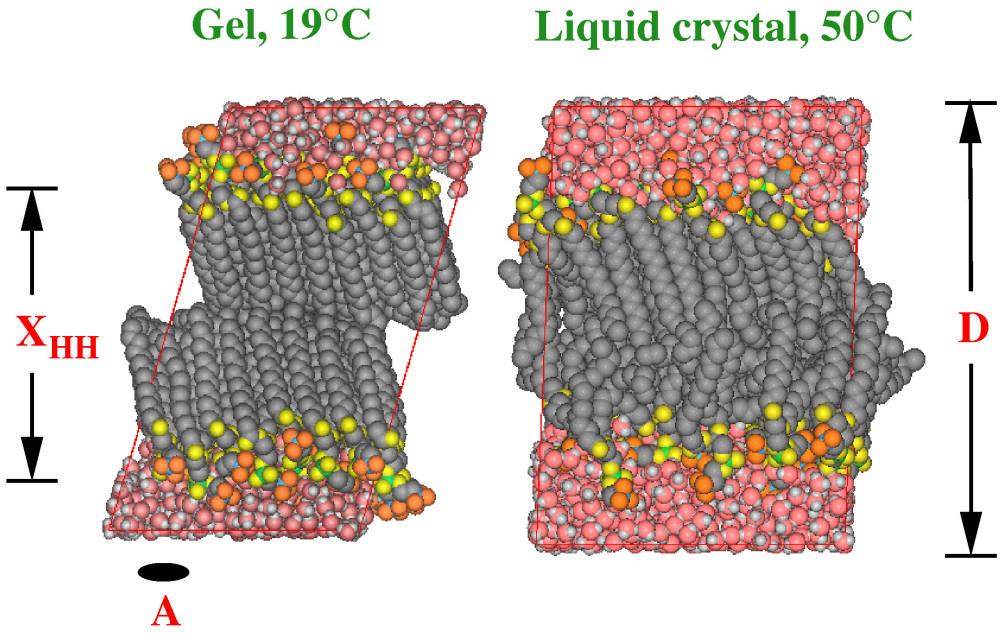

	X–ray [1]	MD [2]	X–ray [3]	MD [4]
A (Å^2)	47.2	45.8	62.9	61.8
D (Å)	63.4	65.2	67.2	67.3
X_{HH} (Å)	45.0	45.6	39.6	38.2

1. Tristram–Nagle et al (1993) Biophys J 64, 97
2. Tu, Tobias & Klein (1996) Biophys J 70, 595
3. Nagle et al (1996) Biophys J 70, 1419
4. Tu, Tobias & Klein (1995) Biophys J 69, 2558

Why Coarse Grain ? *

Atomistic Models

- Empirical potentials - local structures
- Limited system size
- Limited timescale

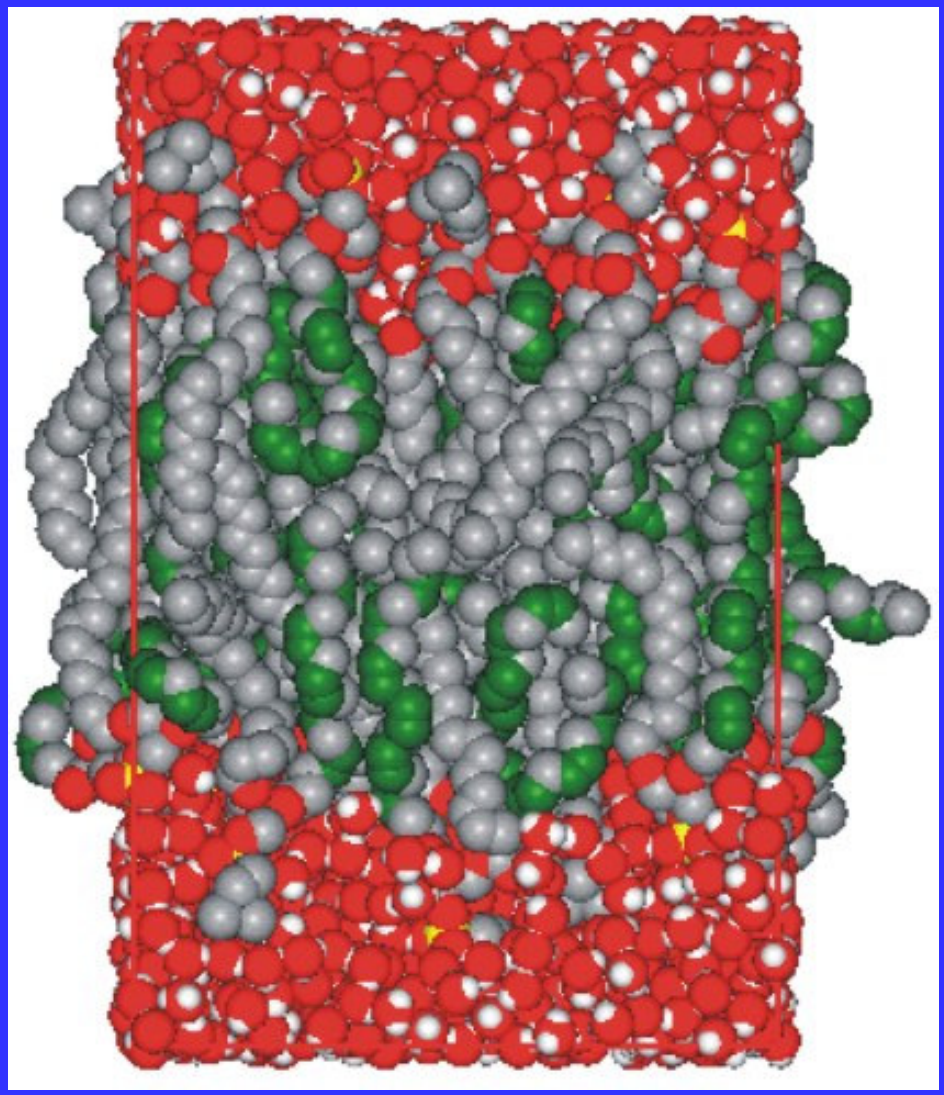

*One can do MD on 100 - 1000 – 10,000 lipids

But one million lipids / μm^2

Coarse Grain Lipid Molecules

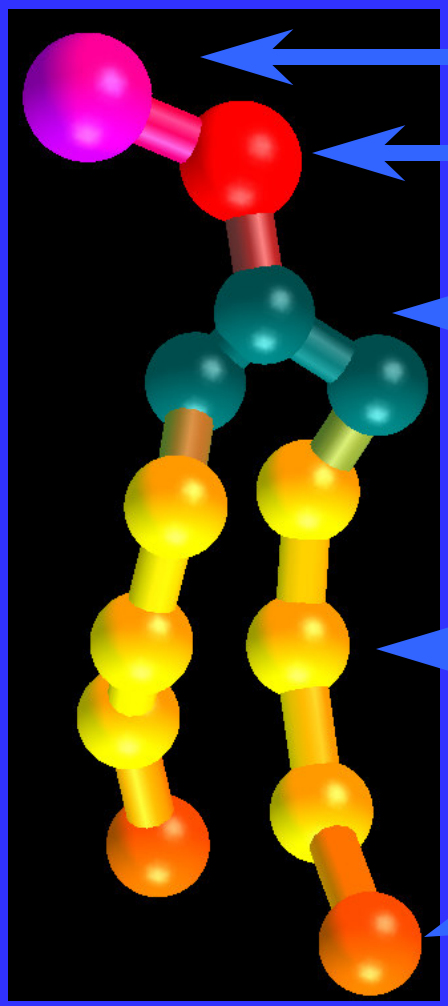

Choline Head Group

Phosphate Group

Glycerol Groups

Acyl Chains

Chain Ends

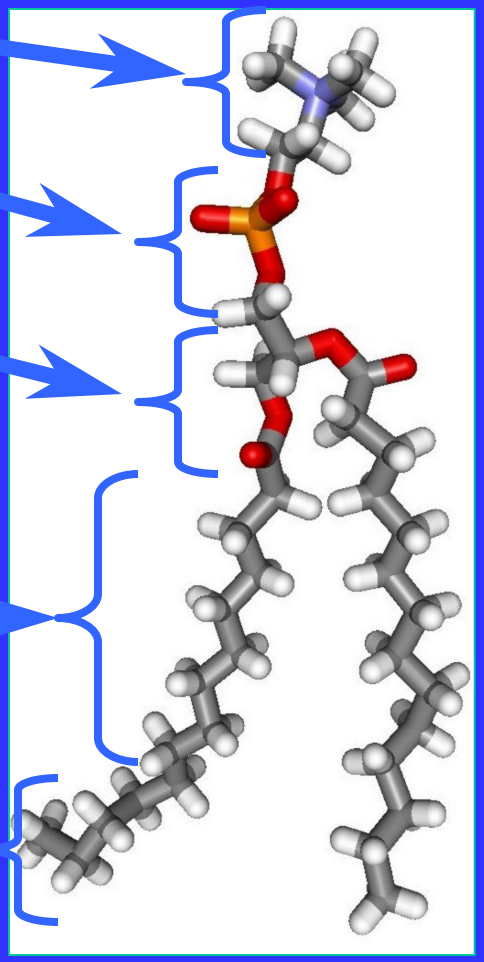

John Shelley, Preston Moore

DMPC-CG 1024 Bilayer

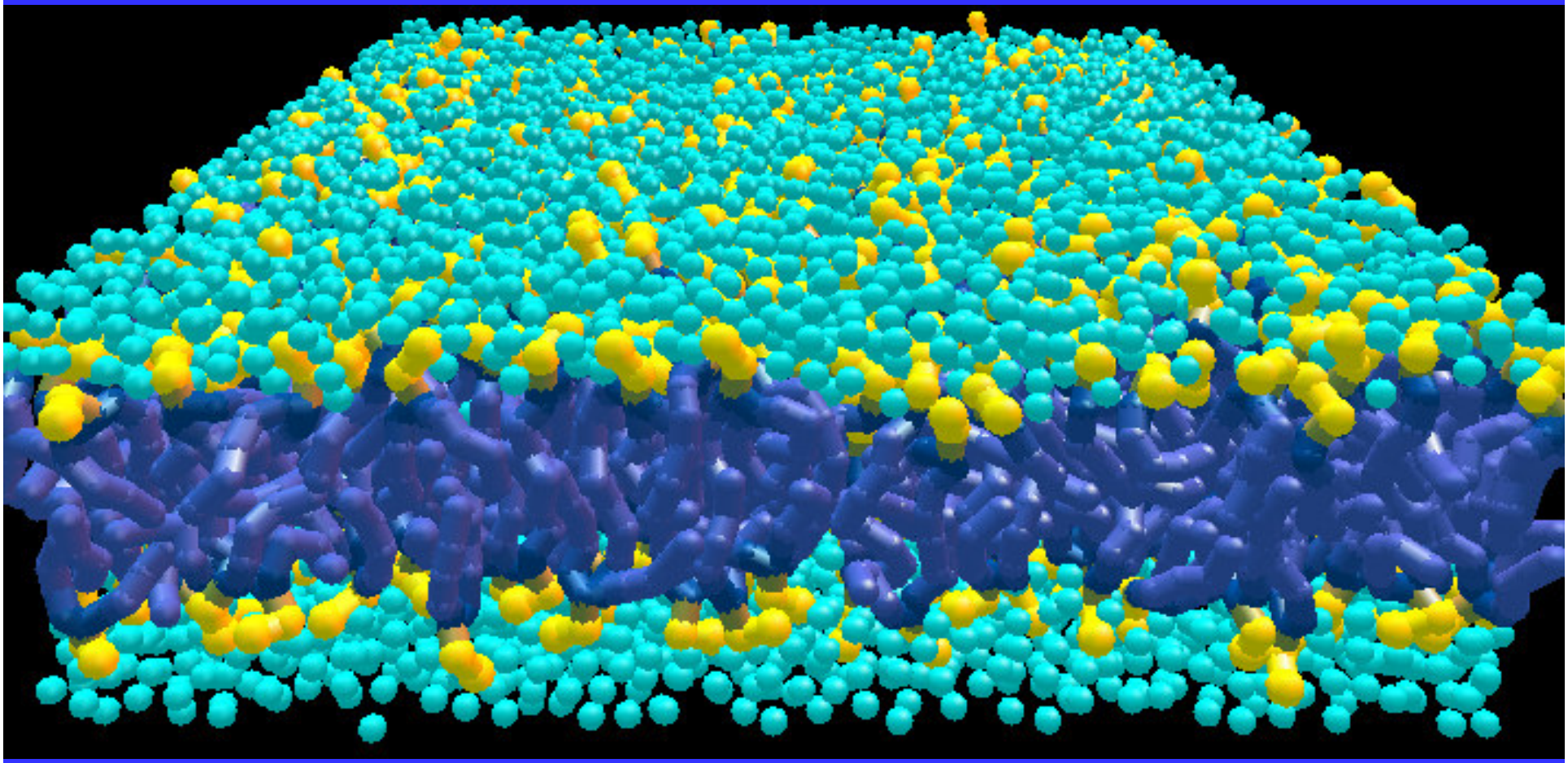

Comp Phys Comm 2002

Understanding Nature's Designs

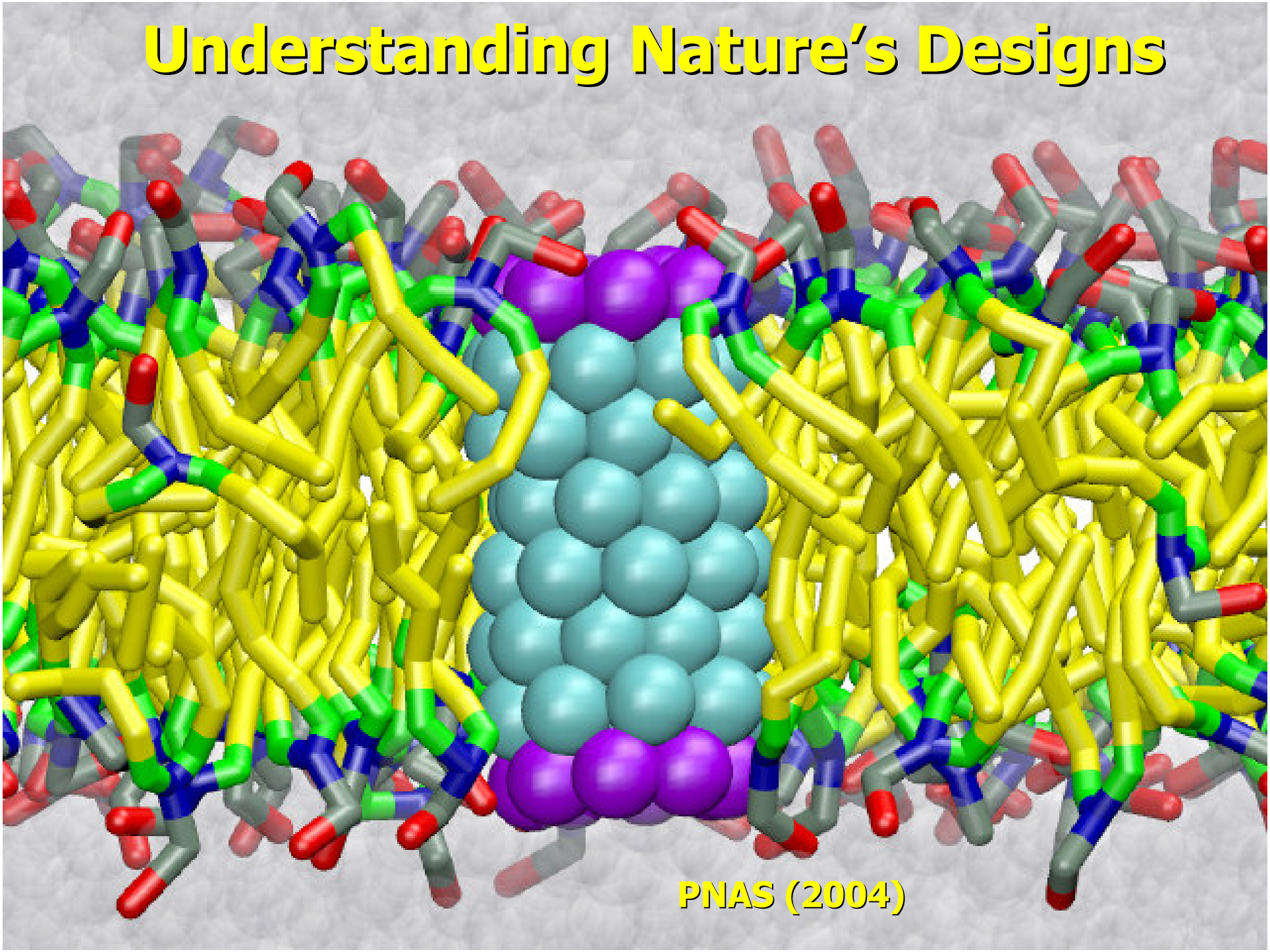

Insertion Synthetic Nanotube into a Membrane

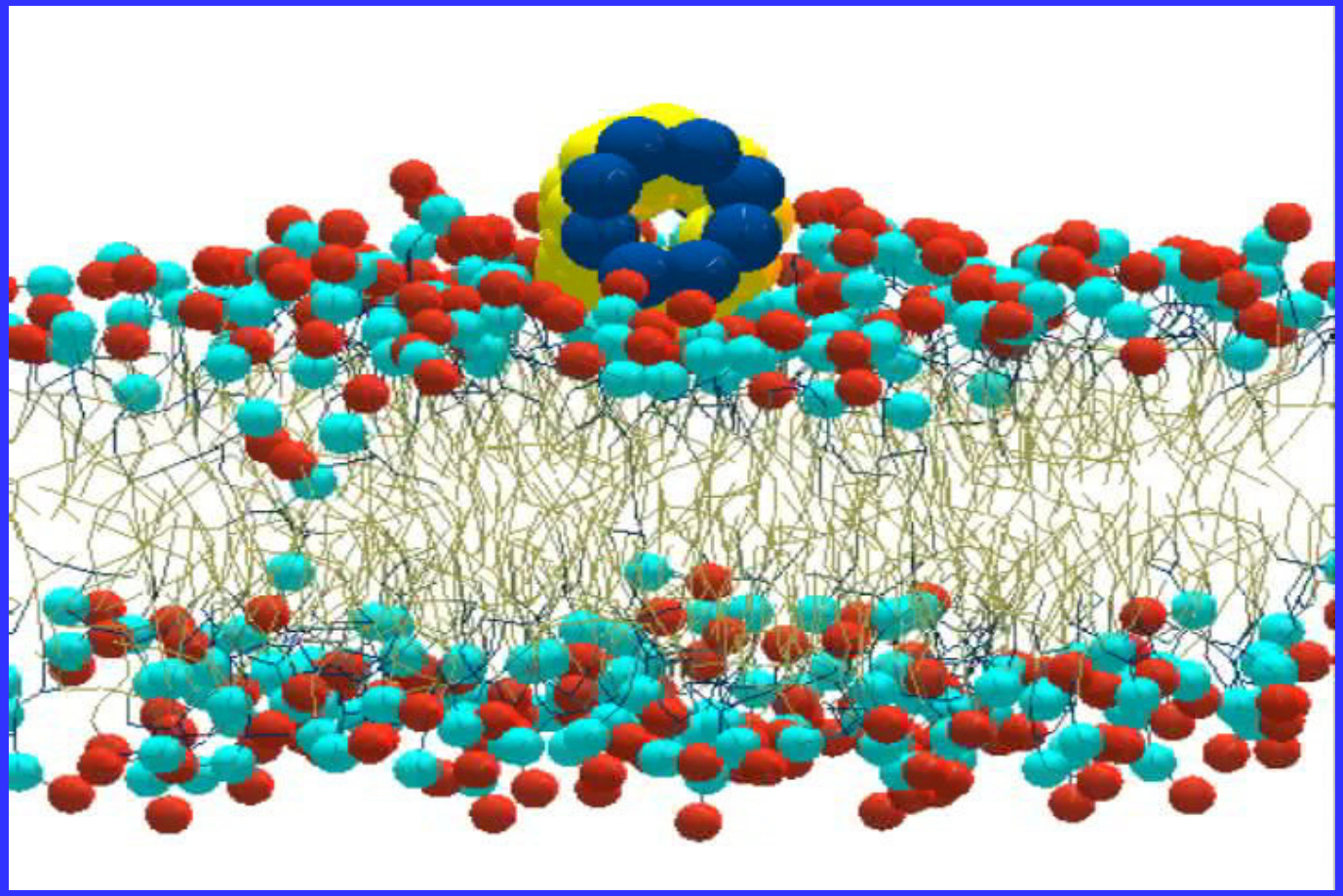

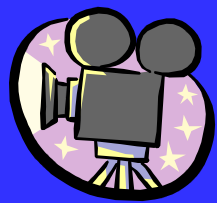

Self-assembly and morphology of block copolymer surfactants

Klein - Discher Students & Postdocs

Center for Molecular Modeling

University of Pennsylvania

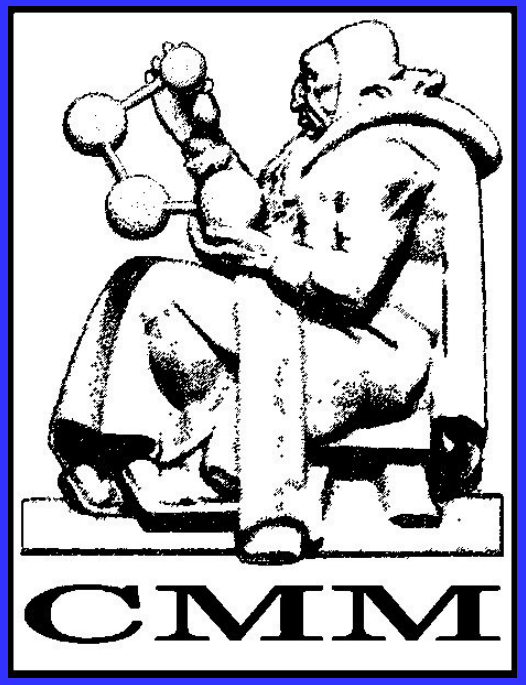

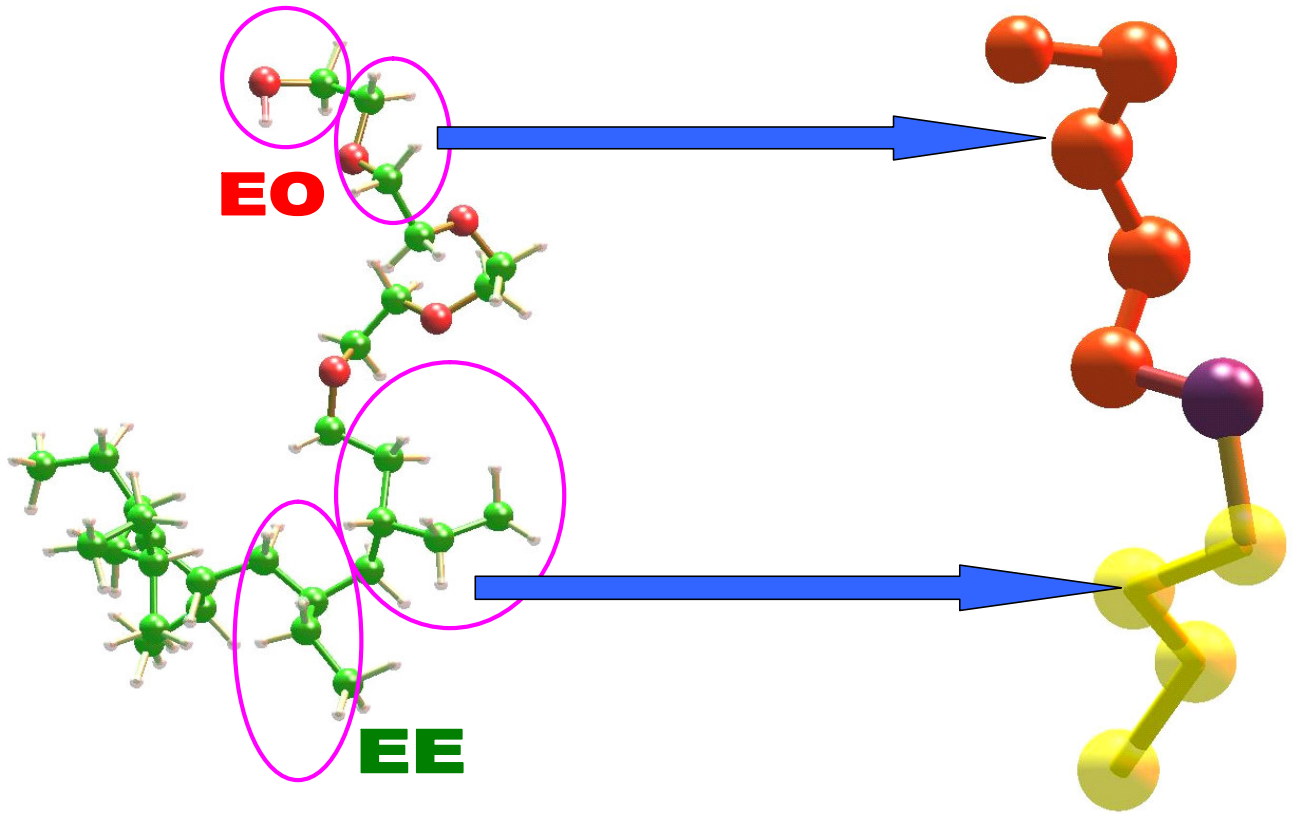

Coarse-grain model for the PEO-PEE diblock copolymer

Summary

Nature Materials (2004)

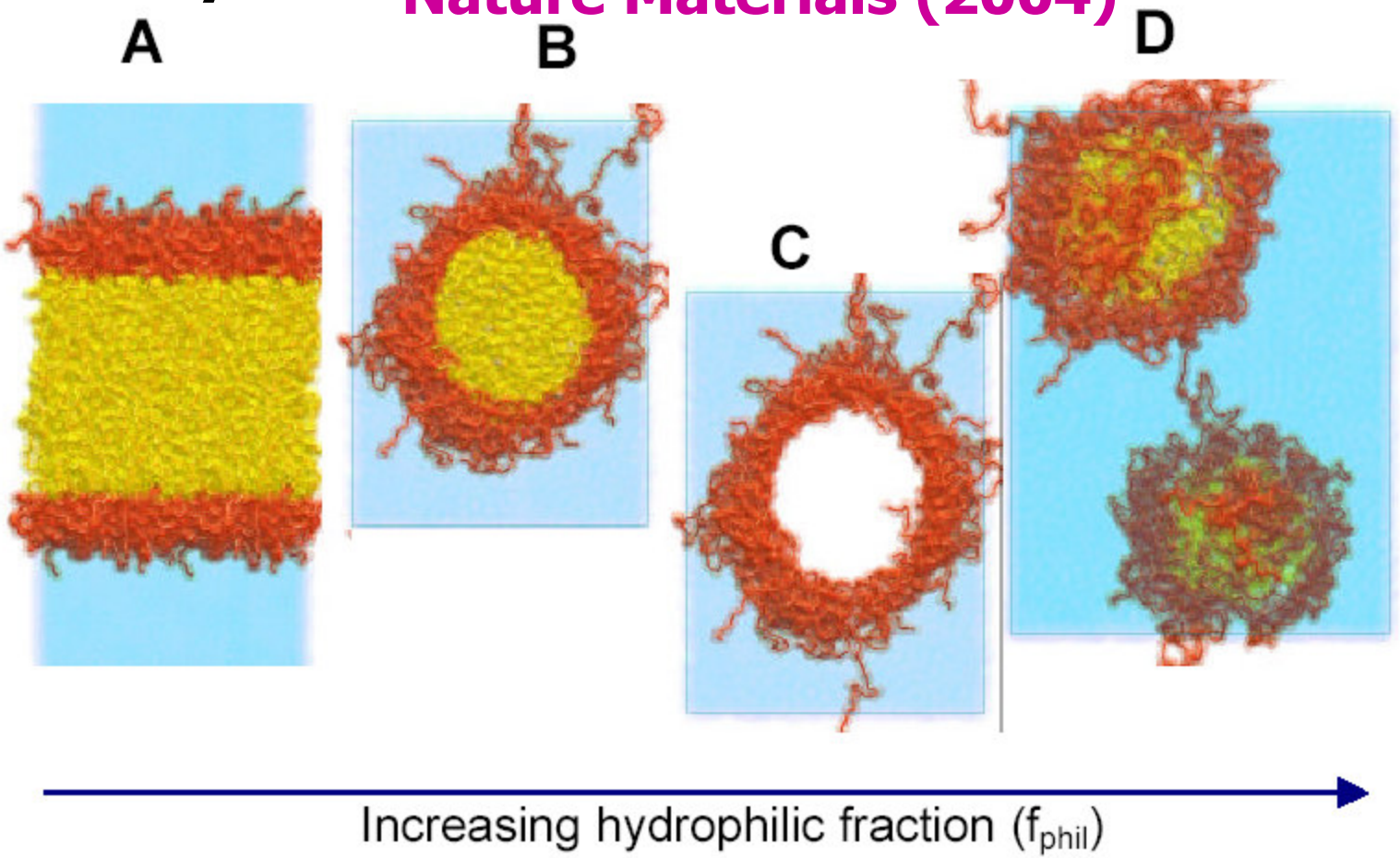

Figure 1: Snap shots taken from CG MD simulations of diblock copolymers in water. Distinct morphologies form spontaneously when the diblock copolymers have different hydrophilic fractions. (A) Bilayer assembly from 30.9% hydrophilic - $EO_{21}EE_{37}$ (B) Cylindrical or worm-like micelle assembled from 51.1% hydrophilic - $EO_{50}EE_{37}$. (C) Same as in (B) showing the hydrophilic EO corona but without the hydrophobic EE core; the cylindrical core extends through the periodic boundaries of the MD simulation. (D) Spherical micelle formed from 65.6% hydrophilic - $EO_{92}EE_{37}$. Color code: hydrophilic EO - red, hydrophobic EE - yellow, water - blue.

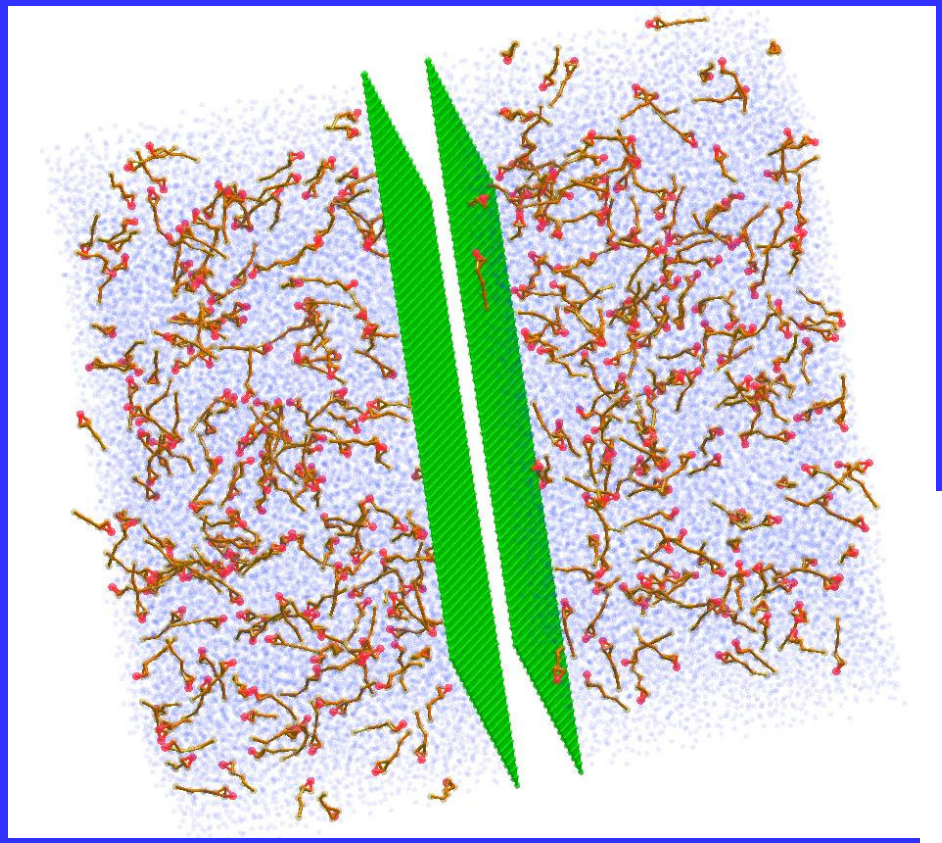

Graphite sheets 100 x 200 Å

425 surfactants (300:1 water)

Random initial condition

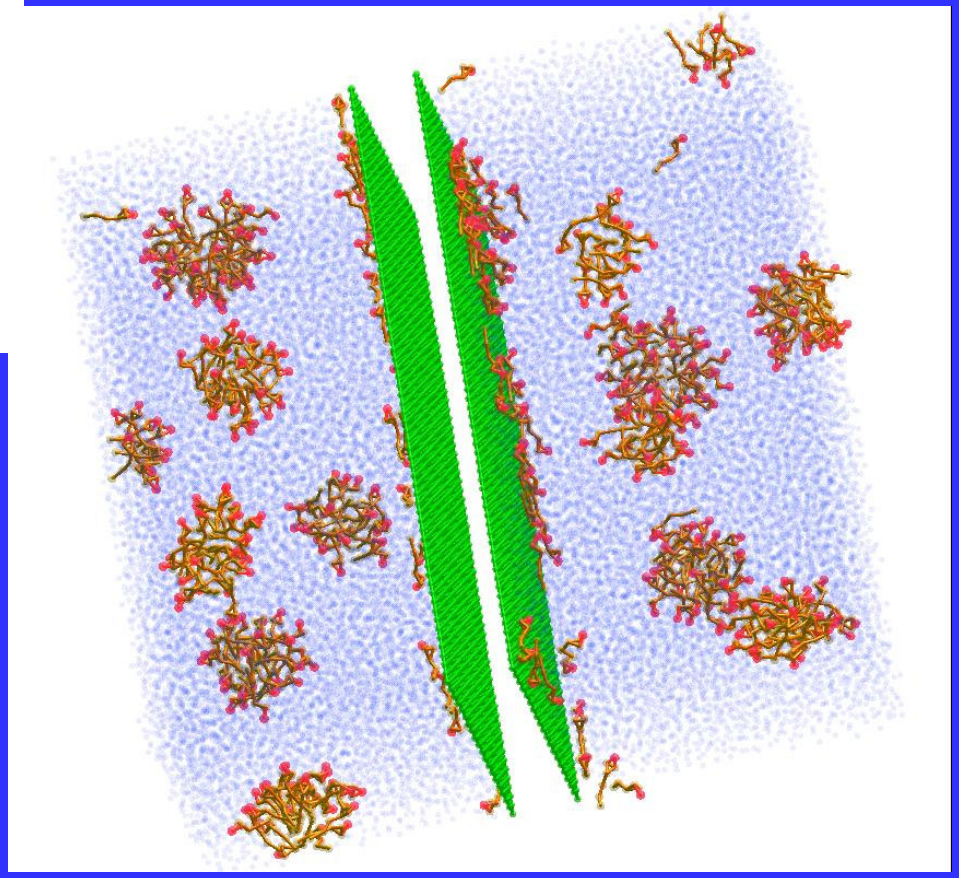

micelles form and surfactant begins to coat surface.